UCRL- 92609
PREPRINT

THREE-DIMENSIONAL SIMULATIONS OF ELECTRON CYCLOTRON HEATING

M. G. McCoy
G. D. Kerbel
R. W. Harvey

This paper was submitted for the 3rd European Workshop on Problems in the Numerical Modeling of Plasmas (NUMOP 85) in Varenna, Italy September 10, 1985.

August 1985

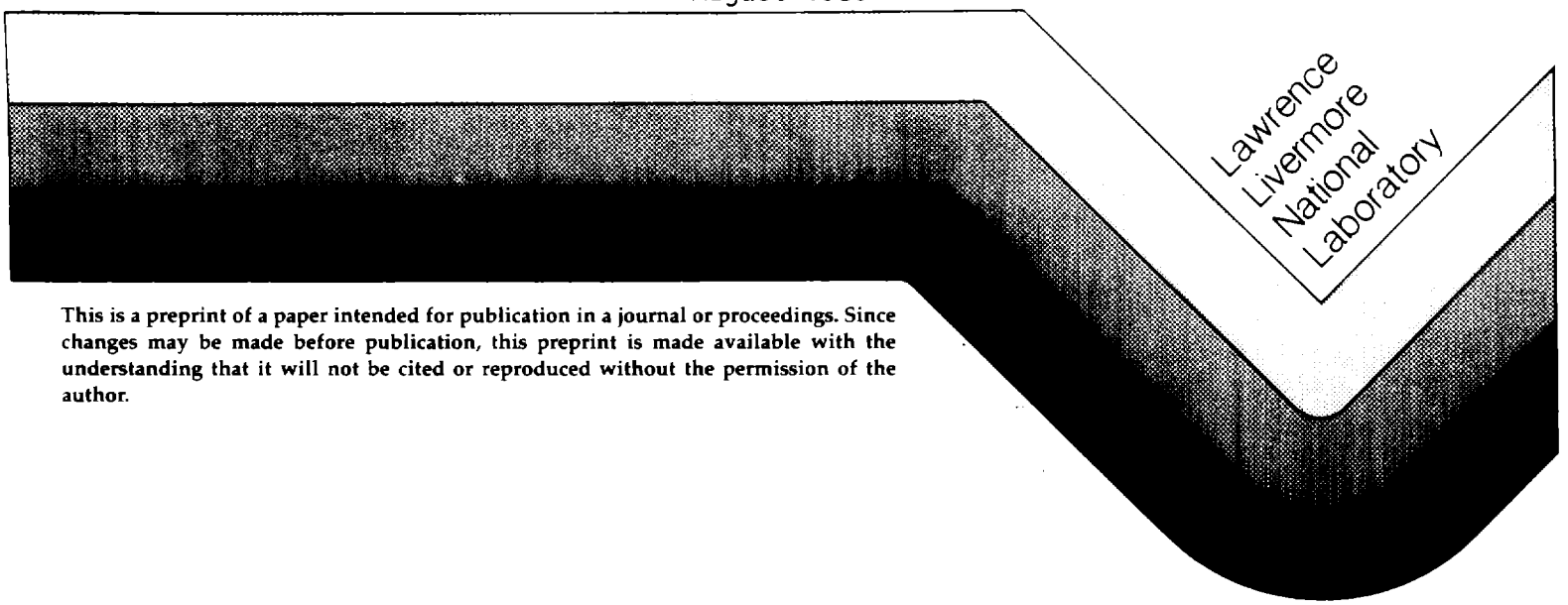

DISCLAIMER

ABSTRACT

Many heating problems in tokamaks are inherently three dimensional, involving the velocity coordinates parallel and perpendicular to the ambient magnetic field and the plasma radial coordinate. We will describe a new three-dimensional, Fokker-Planck/rf quasilinear code. This code is based upon a two-dimensional in velocity space Fokker-Planck code which solves for the distribution evaluated at the outer equatorial plane ($\theta = 0$) of each flux surface in a radial mesh.

The rf energy density ξ satisfies the transport equation

$$\nabla \cdot (\underline{v}_g \xi) = - p_{ABS},$$

where $\underline{v}_g$ is the group velocity of the ordinary or extraordinary wave and p_{ABS} is power absorption obtained using results of the Fokker-Planck code. The rf quasilinear operator is a functional of the wave polarization. Warm plasma relations are used for the group velocity and polarizations.

With knowledge of p_{ABS}, the transport equation is employed to obtain ξ, which is used update the quasilinear diffusion coefficients and resume the Fokker-Planck calculation on the various flux surfaces. The procedure of alternately solving the Fokker-Planck equation and the transport equation is repeated to steady state.

Three-Dimensional Simulations Of Electron Cyclotron Heating *

M. G. McCoy and G. D. Kerbel

National Magnetic Fusion Energy Computer Center
Lawrence Livermore National Laboratory

R. W. Harvey

GA Technologies

I. Introduction

The two dimensional (v=speed, θ=pitch angle) bounce- averaged Fokker-Planck code **CQL** (for **C**ollisional **Q**uasi**L**inear) was developed to simulate a multispecies magnetized plasma whose evolution is governed by an equation with dominant diffusive mechanisms due to small angle Coulomb collisions and wave particle interactions. The starting point is the kinetic equation (with collisions):

$$\frac{\partial f}{\partial t} + \mathbf{v}\cdot\nabla f + \nabla_{\mathbf{v}}\cdot\left(\frac{q}{m}(\mathbf{E}+\frac{\mathbf{v}}{c}\times\mathbf{B})f + \Gamma_c\right) = 0 \tag{1}$$

where Γ_c represents the current density in velocity space due to small angle Coulomb collisions. We are interested in phenomena which evolve on time scales slow with respect to rapid fluctuations associated with the wave, gyro or bounce periods; we therefore average the equation over the appropriate periods, presuming that in order of magnitude

$$\Omega \gg \omega_B \gg \nu_c \sim \nu_{ql} \tag{2}$$

where Ω is the gyro-frequency, ω_B the bounce frequency and ν_c and ν_{ql} the corresponding frequencies for particle- particle and wave-particle interaction.

The model presupposes a symmetric magnetic well in which there occurs nearly recurrent motion of frequency ω_B, with which a gyro-center executes its orbital motion in the varying field structure:

$$\frac{2\pi}{\omega_B} = \tau_B = \oint \frac{ds}{v\cos\theta} = \oint \frac{ds}{v_\parallel}, \tag{3}$$

Here ds is the element of arc length along the magnetic field line associated with the gyro-center motion. The magnetic moment $\mu = mv^2\sin\theta/2B$ and the energy $mv^2/2$ are invariants of the unperturbed motion. Defining $\psi = B(s)/B(0)$, the invariance of μ can be restated as $\sin^2\theta = \psi\sin^2\theta_0$ where θ_0 is the pitch angle coordinate at a fixed point $s = 0$, the bottom of the symmetric magnetic well. Since all orbits pass through this point, a Poincare map there serves well as a representative constants-of-motion space in which to describe the evolution of the distribution on gyro-center orbits of paricle populations. We adopt the notation that a

* Work performed under the auspices of U.S.D.O.E. by LLNL under contract No. W-7405-ENG-48.

subscript $_0$ shall adorn quantities evaluated at this point which hereafter we refer to as the outer equatorial midplane.

Once the appropriate averaging procedures have been applied to (1) the bounce-averaged Fokker-Planck equation which results may be expressed in particle conservation form

$$\begin{aligned}\left(\frac{\delta\lambda\mathcal{F}_0}{\delta t}\right)_{cql} &= -\nabla_{\mathbf{v}_0}\cdot\hat{\Gamma}_0 \\ &= \gamma\Big(\frac{1}{v_0^2}\frac{\partial}{\partial v_0}\Big(A_0 + B_0\frac{\partial}{\partial v_0} + C_0\frac{\partial}{\partial\theta_0}\Big) + \frac{1}{{v_0}^2\sin\theta_0}\frac{\partial}{\partial\theta_0}\Big(D_0 + E_0\frac{\partial}{\partial v_0} + F_0\frac{\partial}{\partial\theta_0}\Big)\Big)\mathcal{F}_0 \quad (4)\\ &= \gamma\Big(\frac{1}{v_0^2}\frac{\partial\mathcal{G}_0}{\partial v_0} + \frac{1}{{v_0}^2\sin\theta_0}\frac{\partial\mathcal{H}_0}{\partial\theta_0}\Big)\end{aligned}$$

Here $\gamma = 4\pi z^4 e^4/m^2$ and the coefficients $A_0 - F_0$ represent the sum of particle-particle, wave-particle and small amplitude steady electric field effects, appropriately bounce-averaged. The quantity $\lambda = v_0\cos\theta_0\tau_B$ is a geometric length factor and the conserved quantity, the number of particles on a field line, is

$$\begin{aligned}0 = \frac{\partial N}{\partial t} &= \int d^3v_0\, v_0\cos\theta_0\tau_B\left(\frac{\delta\mathcal{F}}{\delta t}\right)_{cql} = \int d^3v_0\, v_0\cos\theta_0\tau_B\langle\langle\nabla_{\mathbf{v}}\cdot\hat{\Gamma}\rangle\rangle \\ &= \int d^3v_0\,\nabla_{\mathbf{v}_0}\cdot\hat{\Gamma}_0\end{aligned} \quad (5)$$

This invariant is enforced in the code down to roundoff.

Many heating problems in tokamaks are inherently four dimensional, involving not only the velocity space coordinates (v_0,θ_0), but the spacial coordinates (r,θ_p) as well. Recently, we have generalized **CQL** to **CQL3D** by adding effects involving these coordinates. The new code solves the Fokker-Planck equation at a number of flux surfaces in parallel and computes the local power absorption P_{abs} as a function of minor radius r and poloidal angle θ_p. Coupling between the various flux surfaces is achieved through the solution of a transport equation for $\mathcal{E}_{\mathbf{k}}$, the RF energy density

$$\nabla\cdot(\mathbf{v}_g\mathcal{E}_{\mathbf{k}}) = -P_{abs} \quad (6)$$

where $\mathbf{v}_g$ is the group velocity of the ordinary or extra- ordinary wave. The generation of $\mathcal{E}_{\mathbf{k}}$ allows the recalculation of self-consistent RF coefficients and will be discussed in detail in Section III.

II. Numerical Features of CQL

II.A The Fokker-Planck equation (4) requires the generation of the six coefficients $A_0 - F_0$ which represent the accumulated effects of all relevant physical processes. Kerbel and McCoy[3] have discussed the generation of the quasilinear coefficients $B_{0_{ql}} - F_{0_{ql}}$. In that case, the relevant bounce-averages can be evaluated analytically in the asymptotic limit $\Omega\tau_B \to \infty$ since the region of wave-particle resonant interaction is localized. On the other hand, collisions occur everywhere along a particle trajectory and for non-linear calculations the Fokker-Planck

coefficients $A_{0_c} - F_{0_c}$ must be computed through the numerical bounce-average of the local Fokker-Planck coefficients:

$$A_0 = \lambda\langle\langle A\rangle\rangle; \quad B_0 = \lambda\langle\langle B\rangle\rangle; \quad C_0 = \lambda\langle\langle \frac{\cos\theta}{\sqrt{\psi}\cos\theta_0} C\rangle\rangle$$
$$D_0 = \lambda\langle\langle \frac{\cos\theta}{\psi\cos\theta_0} D\rangle\rangle; \quad E_0 = \lambda\langle\langle \frac{\cos\theta}{\psi\cos\theta_0} E\rangle\rangle; \quad F_0 = \lambda\langle\langle \frac{\cos^2\theta}{(\sqrt{\psi})^3\cos^2\theta_0} F\rangle\rangle \tag{7}$$

The calculation of the local coefficients is well known[1] and will not be described here, except to say that the Rosenbluth potentials and the distribution functions are expanded in Legendre series. The local coefficients $A - F$ are evaluated at a pitch angle θ such that the particle's orbit traced back to the midplane intersects at the midplane mesh point θ_0. This eliminates the need for interpolation during the bounce-average, which is reduced to a trival addition. Thus for $\theta_0(i), v_0(j)$ we have the bounce-average of a function $g(v, \theta, s)$ approximated by

$$\tau_B(v_j, \theta_i)\langle\langle g(v, \theta, s)\rangle\rangle\Big|_{v_j,\theta_j} = \int_0^{s_B} \frac{ds}{v_j\cos\theta(\theta_i, s)} g\big(v_j, \theta(\theta_i, s), s\big)$$
$$\cong \sum_l g_l \, d\tau_B(j, i, l) \tag{8}$$

and s_B is the bounce point and the bounce time on the left hand side of (8) is given by the sum

$$\tau_B(v_j, \theta_i) = \sum_l d\tau_B(j, i, l).$$

II.B Conservation of particle density is achieved by a numerical analogue of (4). The only difficulty that presents itself is to be found at the trapped/passing boundary. Here a separatrix divides the particles on banana orbits from those on passing orbits and τ_B has a logarithmic singularity. The ordering (2) breaks down in a small boundary region in the neighborhood of this feature. The proper boundary condition is that of flux balance: the total number of particles leaving the passing regions should equal the sum of the number of particles entering the trapped region and the boundary layer. This requires knowledge of the average value of $\lambda = v_{\|0}\tau_B \sin\theta_0 \, d\theta_0$ in the boundary region, and this is evaluated through a series expansion for τ_B involving elliptic integrals and a Hastings polynomial expression for K and E, the complete elliptic integrals.

II.C Time advancement is currently achieved by a splitting scheme, which while adequate for time dependent calculations on a single flux surface is probably inadequate for multi-flux surface calculations. The program described byO'Brien et.al.[5] uses a Gaussian elimination method which is presently being adapted to this code to allow fully implicit differencing.

III. Three Dimensional Generalization - CQL3D

The three dimensional version **CQL3D** resulted from a desire to obtain a global picture of electron distribution function evolution throughout the plasma cross section in the presence of ECRH excitation. There are two major components to the calculation. The first is the computation by **CQL**, run in parallel at a number of neighboring flux surfaces, of $\mathcal{F}_0(v,\theta,r;t)$ and $P_{abs}(r,\theta_p)$. This latter power is that RF power absorbed in a given poloidal neighborhood. The second component provides the linkage between the flux surfaces themselves through a solution of the transport equation for RF energy density $\mathcal{E}_{\mathbf{k}}$. The quantity $\mathcal{E}_{\mathbf{k}}$ may be used to determine E_- the right hand component of the electric field. This allows for the recalculation of the four quasilinear coefficients and thus feeds back into **CQL**. We will first describe the model used for the calculation of the wave damping and $\mathcal{E}_{\mathbf{k}}$, then touch upon the coupling of **CQL** with the wave damping model, with an emphasis on parallelization.

III.A For simplicity, in this report we consider only the component of the group velocity in the $\hat{\mathbf{e}}_R$ (major radial) direction-rays propagate parallel to the equatorial plane (Fig. 1). RF power flowing into horizontal ray channels is constant from $z = 0$ to $z = z_1$ and then decreases linearly to zero at $z = z_2$. Up/down symmetry is assumed. This model avoids some of the complexities that would arise if the group velocity $\mathbf{v}_g$ were general, and provides a physically reasonable and numerically tractable initial approach to the problem.

The total RF antenna power is specified as is the mode type, ie. O-mode or X-mode. Also required are the local background electron and ion temperature and density, the parallel wave refractive index and the wave frequency. A warm plasma dispersion relation subroutine is used to determine the group velocity $\mathbf{v}_g$, the energy density factor

$$\mathbf{E}_f = \frac{1}{16\pi}\left\{\frac{\mathbf{B}\cdot\mathbf{B}^*}{|\mathbf{E}|^2} + \frac{\mathbf{E}}{|\mathbf{E}|}\cdot\frac{\partial\omega\mathbf{K}}{\partial\omega}\cdot\frac{\mathbf{E}^*}{|\mathbf{E}|}\right\} \tag{9}$$

and the fraction of right-hand polorization $|E_-/E|^2$. Here $\mathbf{K}$ is the warm plasma dispersion tensor and as mentioned before, we take $\mathbf{v}_g \rightarrow \mathbf{v}_g\cdot\hat{\mathbf{e}}_R\hat{\mathbf{e}}_R$. The transport equation for energy density (6)

$$\nabla\cdot(\mathbf{v}_g\mathcal{E}_{\mathbf{k}}) = -P_{abs}(\mathcal{E}_{\mathbf{k}}) \tag{10}$$

is now employed to obtain $\mathcal{E}_{\mathbf{k}}$. In the current approximation $\nabla\cdot \equiv \partial/\partial R + 1/R$: Then using the results of the wave characteristics package we obtain

$$E_-^2(R,z) = \frac{1}{\mathbf{E}_f(R,z)}\mathcal{E}_{\mathbf{k}}(R,z)\left|\frac{E_-}{E}\right|^2(R,z) \tag{11}$$

Coupling with the kinetic equation solved by **CQL** is achieved through the updating of the coefficients $B_{0_{ql}} - F_{0_{ql}}$. The electric field $E_-(R,z)$ is interpolated onto the (r,θ_p) mesh. Then, as described byKerbel and McCoy[3] , **CQL** can update the quasilinear coefficients and recompute $P_{abs}(r,\theta_p)$ in order to bring these quantities closer to self consistency. The power is reinterpolated to (R,z) and the entire solution procedure for E_- is repeated to convergence, with relaxation over previous iterates for $\mathcal{E}_{\mathbf{k}}$. Generally, less than five iterations are required.

Figs.(2-3) represent contours of $P_{abs}(R,z)$ and $E_{-}(R,z)$ for a case of inside launch X-mode. The wave frequency was chosen so that the resonant layer would occur at $R = R_0$; this represents a case in which all the wave energy is deposited in a single pass.

III.B The high degree of canonical parallelization present in this formulation, coupled with the extensive memory requirements inherent in electron kinetic equations makes **CQL3D** likely grist for the CRAY-2 mill.

Clearly, once the quasilinear coefficients have been defined on the various flux surfaces, the distribution functions may be advanced in parallel (over the radial coordinate) until it seems necessary to update the RF wave field amplitude. The flow chart Fig. 4 describes the calculation:

1) Initialization (can be done in parallel): The quasilinear setup calculation generates the array of normalized interaction strengths, $\bar{b}_0$, and the packed array of resonance localization weights, $W(\theta_p)$:

$$B_{0_{ql}} = \bar{b}_0 \int d\theta_p W(\theta_p)\, \mathcal{E}_{\mathbf{k}}(\theta_p)$$

The quantities $\bar{b}_0$ and W are functions of orbit invariants v_0, θ_0 as well as wave field parameters $\omega, k_{\|}, k_{\perp}$ and wave polorization at resonance. The quantity $\mathcal{E}_{\mathbf{k}}(\theta_p)$, the spectral energy density, is calculated as a time dependent quantity, using the wave depletion model.

2) Initialization (not in parallel): Solve the warm plasma dispersion relation at all points on the (R,z) grid.

3) Iteration procedure to compute $B_{0_{ql}} - F_{0_{ql}}$ (can be partially done in parallel): Solution of transport equation (6) is not done in parallel, however the calculation of $B_{0_{ql}} - F_{0_{ql}}$ in **CQL** can be multiprocessed.

4) Fokker-Planck calculation (can be done in parallel): Both the determination of the collisional coeficients and the advancement of $\mathcal{F}_0$ can be done in parallel.

The code **CQL3D** does not attempt to keep all arrays in core simultaneously. While this would be possible for some runs on the CRAY-2, it would preclude the use of the code on any other machine. Instead, any relevant arrays which are local to a given flux surface are stored on disk and retrieved only when needed.

IV. Sample calculation

An example has been chosen to illustrate the marked variation of the RF heated electron distribution versus plasma radius. Plasma parameters are chosen pertaining to the Doublet III ECH experiment,[6] viz., 60 GHz inside launch of X-mode power into a 50 cm, aspect ratio $A = 3$ plasma which has central electron density $n_e = 2 \times 10^{13}\,\mathrm{cm}^{-3}$ parabolic profile.

We are considering the case corresponding to the RF power deposition illustrated in Figs. 2-3. This is after 2 msec of 1 V one-turn applied electric potential, followed by 1 MW of RF power for 4 msec. The average electron energy changes as shown in Fig. 5. The electrons have been evolved with the nonlinear collision operator with no sinks of energy, so the plasma temperature rises (indefinitely).

The electron distribution function has been calculated on fifteen radial mesh points. In Fig. 6 contour diagrams of the distributions obtained at $r/a = 0.1$, .23 and .5 are shown. Near the plasma center, Fig. 6(a), the distortion of the tail is primarily due to the applied D.C. electric field, even though the .8 $\mathrm{W/cm^3}$ Ohmic and RF powers to the distribution are aproximately equal. The Doppler shifted parallel resonant energy on the outer equatorial resonant surface is only 1.2 keV in this case, so most of the RF heating is in the bulk. The RF effect has been further reduced by the combined effects of energy deposition on the outer flux surfaces, and the dispersive effects of the plasma which gives relatively little right-hand polarized energy.

The distribution at $r/a = .23$ in Fig. 6(b) illustrates a tail temperature which slowly increases with energy. The contours would be increasingly closely spaced with energy for a Maxwellian distribution. The resonant parallel energy is 5.7 keV in this case. RF power deposition equal to 1.5 $\mathrm{W/cm^3}$ is approximately 3 times the Ohmic power.

Further out in the plasma at $r/a = .5$, shown in Fig. 6(c), the effect of the RF on the distribution is entirely in the tail. The RF power deposition is only about .001 $\mathrm{W/cm^3}$, but this gives a marked effect beyond the 23 keV resonant energy.

Future work will include modules to calcululate the soft-X-ray and electron cyclotron emission spectra from the electron distributions, thus facilitating direct comparison with experiments.

References

[1]J. Killeen, G. D. Kerbel, M. G. McCoy, and A. A. Mirin, *Computational Methods for Kinetic Models of Magnetically Confined Plasmas*, Springer-Verlag, to be published.

[2]G. D. Kerbel and M. G. McCoy, *Kinetic Theory and Simulation of Multi-Species Plasmas in Tokamaks Excited With ICRF Waves*, UCRL-92062, LLNL, (1984); to be published Phys. Fluids (November, 1985).

[3]G. D. Kerbel and M. G. McCoy, *Collision Broadened Resonance Localization in Tokamaks Excited with ICRF Waves*, Varenna, 1985.

[4]J. Y. Hsu, V. S. Chan, and F. W. McClain, Phys. Fluids, **26**, 11 (1983).

[5]M. O'Brien, M. Cox, D. Start, *Fokker-Planck Calculations Of RF Heating In Tokamaks*, Varenna, 1985.

[6]R. Prater, GA Technologies, private communication.

Figure Captions

FIG. 1. **Geometry of wave damping model** Rays propagate parallel to the equatorial plane. RF power flowing into horizontal ray channels is uniform for $-z_1 < z < z_1$ and decreases linearly to zero at $z = \pm z_2$.

FIG. 2. **Contours of $P_{abs}(R,z)$, the local wave power absorption.** The contours span three orders of magnitude and represent evenly spaced increments in $\ln 10^3$.

FIG. 3. **Contours of E_-, the right hand component of the wave electric field.** Contours span three orders of magnitude.

FIG. 4. **Flow chart describing the structure of CQL3D.** Blocks occuring on the same horizontal line are independent and can be computed in parallel (multi-tasked).

FIG. 5. **Average electron energy.** Electron energy as a function of minor radius at time $t = 0$ and $t = 6$msec.

FIG. 6. **Electron distribution function $\mathcal{F}_e$.** Contours of $\mathcal{F}_e$ over 13 orders of magnitude after 6msec of 1V one-turn applied electric potential followed by 4msec of RF wave excitation. The three radial positions correspond to (a) $r/a = .1$, (b) $r/a = .23$, and (c) $r/a = .5$.

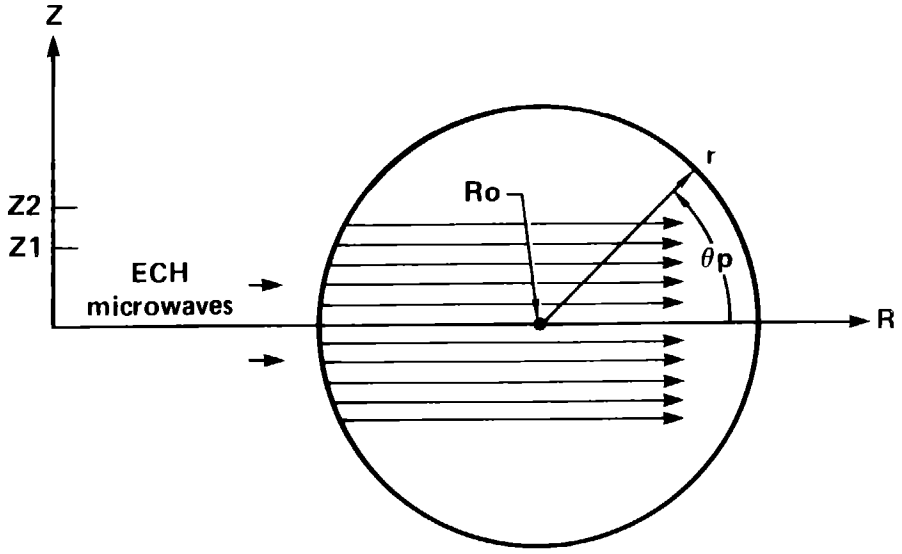

Figure 1

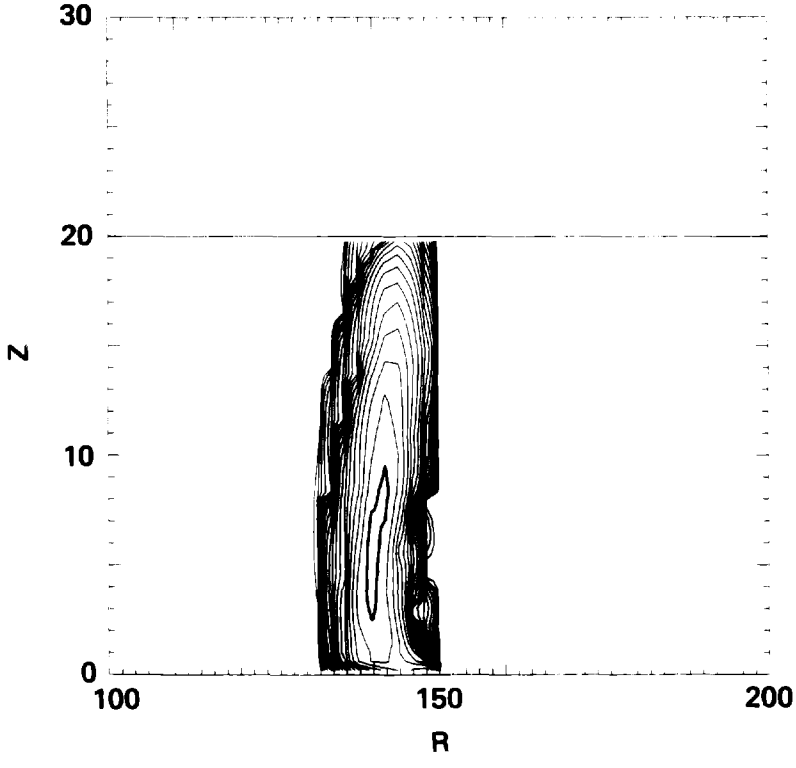

Figure 2

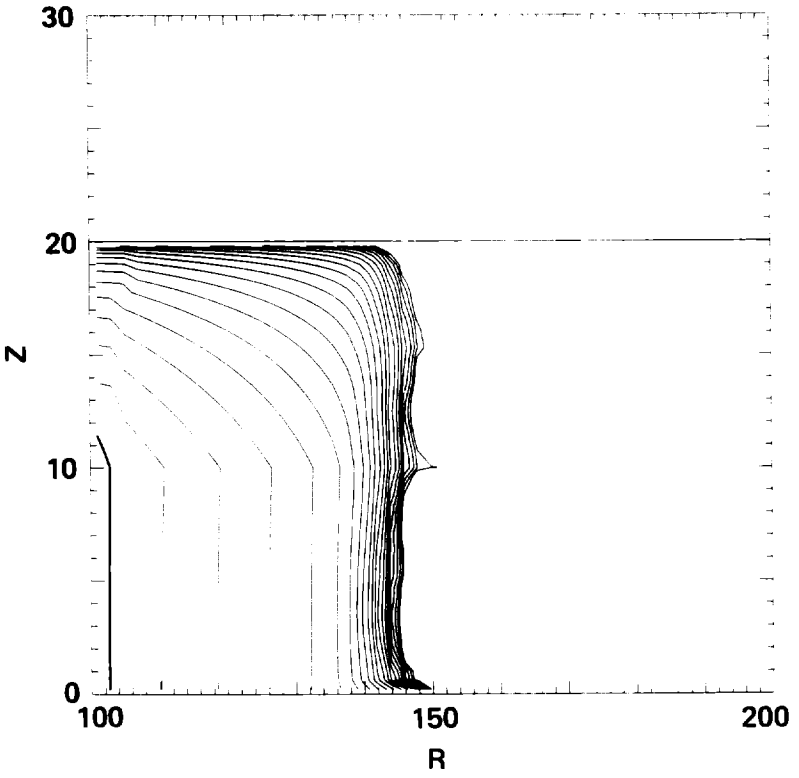

Figure 3

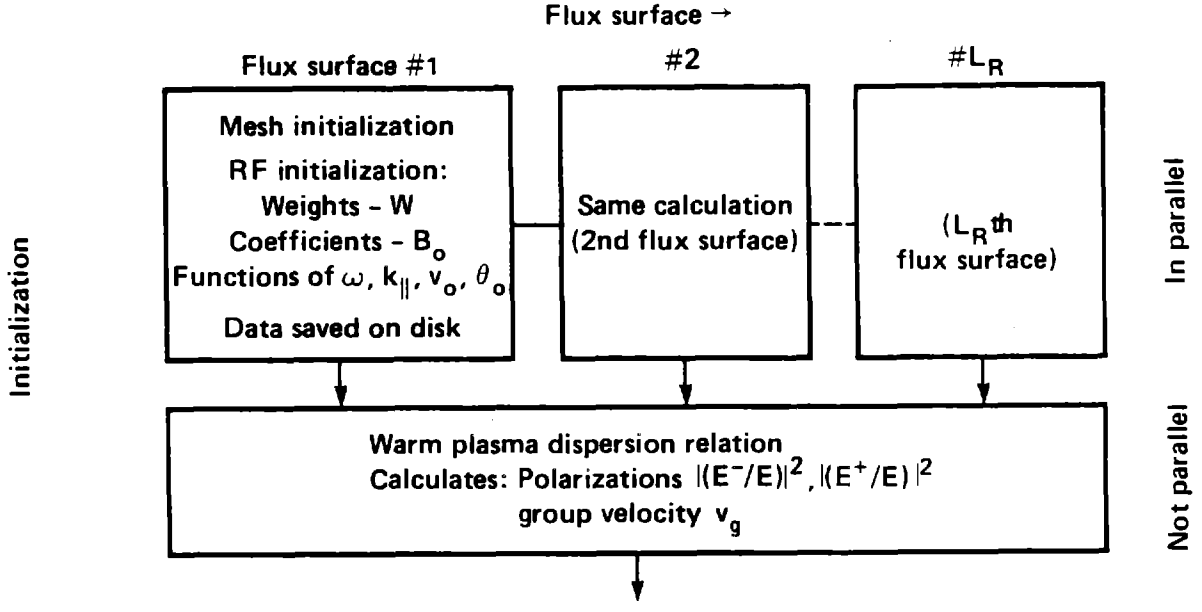
Flux surface →
Flux surface #1
#2
#L_R
Mesh initialization
RF initialization:
Weights - W
Coefficients - B_o
Functions of ω, $k_{||}$, v_o, θ_o
Data saved on disk
Same calculation
(2nd flux surface)
(L_Rth
flux surface)
Warm plasma dispersion relation
Calculates: Polarizations $|(E^-/E)|^2$, $|(E^+/E)|^2$
group velocity v_g
Initialization
In parallel
Not parallel

Figure 4

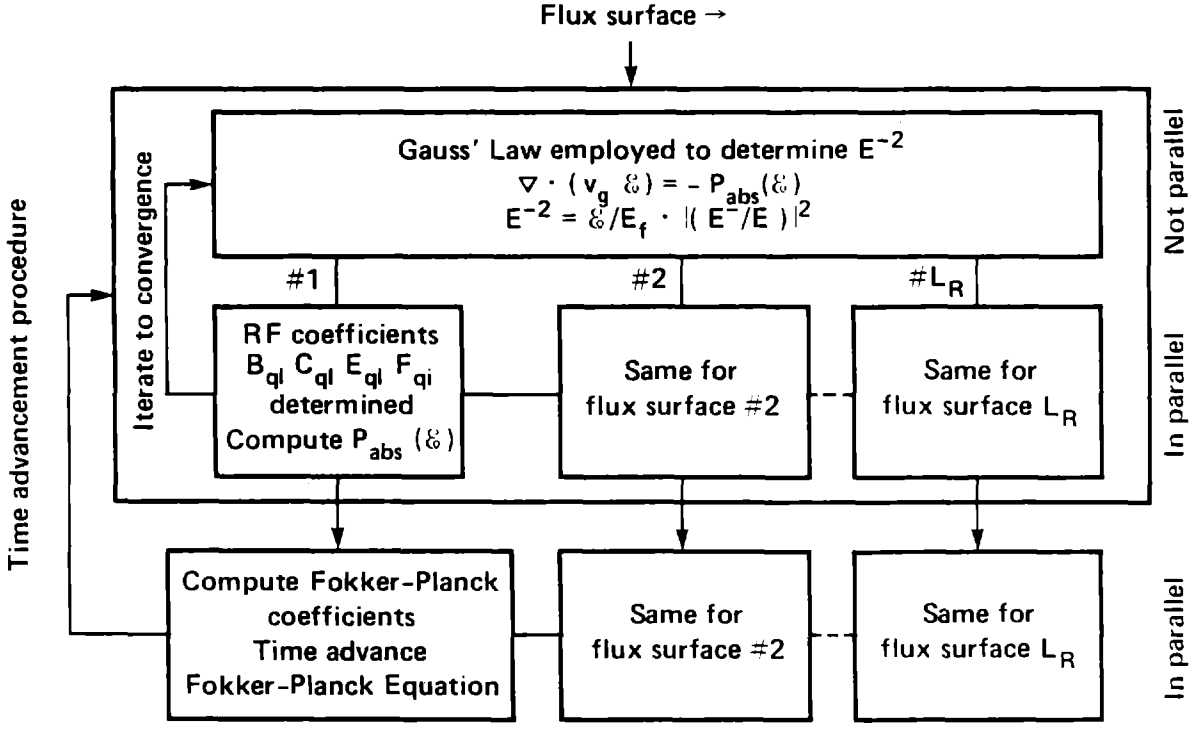

Figure 4 (Continued)

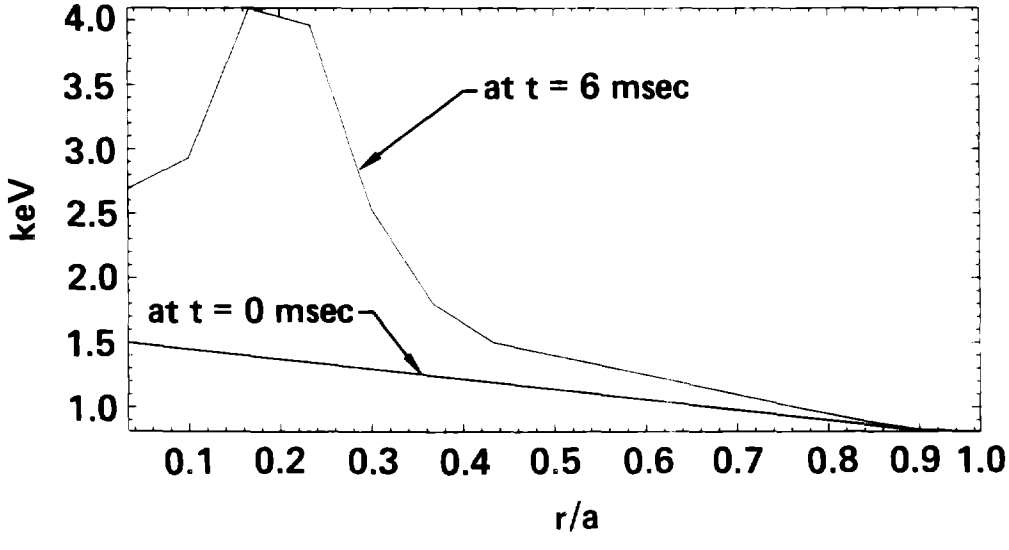
4.0
3.5
3.0
2.5
2.0
1.5
1.0
keV
at t = 6 msec
at t = 0 msec
0.1
0.2
0.3
0.4
0.5
0.6
0.7
0.8
0.9
1.0
r/a

Figure 5

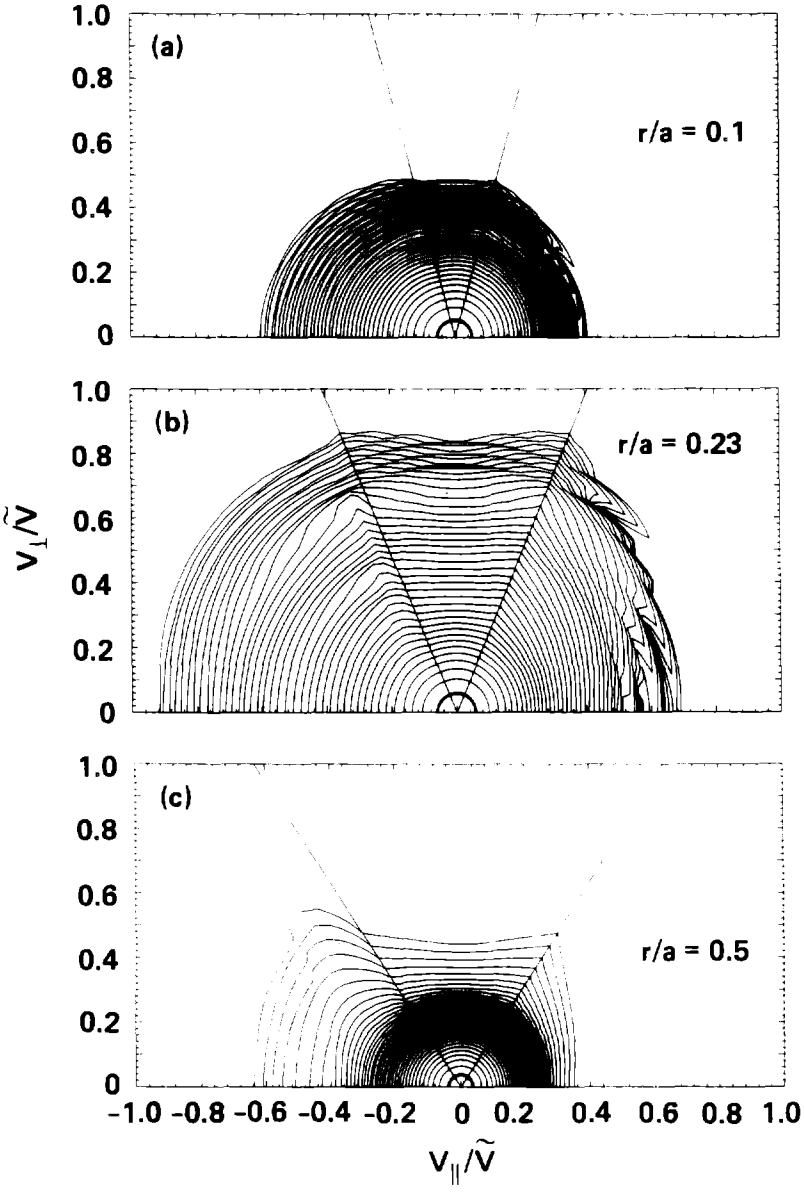
(a)
r/a = 0.1
(b)
r/a = 0.23
(c)
r/a = 0.5
1.0
0.8
0.6
0.4
0.2
0
-1.0 -0.8 -0.6 -0.4 -0.2 0 0.2 0.4 0.6 0.8 1.0
$v_\perp/\tilde{v}$
$v_\parallel/\tilde{v}$

Figure 6